

# Structural and Bonding Trends among the $B_7C_1^{1-}$ , $B_6C_2$ , and $B_5C_3^{1+}$

Sung Soo Park

Department of Physics, Atmospheric Sciences, and General Science, Jackson State University, Jackson, MS 39217, USA

\*E-mail: sung.s.park@ccaix.jsums.edu

Received August 4, 2004

Equilibrium geometries, electronic structures, and energies of borocarbon clusters (binary compounds of carbon and boron), an unexplored class of molecules with highly unusual characteristics and potential for further development, have been investigated by means of B3LYP/6-311+G\* density functional theory computations. A large number of  $B_7C_1^{1-}$ ,  $B_6C_2$ , and  $B_5C_3^{1-}$  clusters with planar and non-planar monocyclic and polycyclic rings, as well as cage structures, have been systematically studied. Unexpectedly, planar forms are predicted not only to be the most stable structures, but also, in many cases, to have unprecedented planar heptacoordinate boron (p-heptaB) and planar heptacoordinate carbon (p-heptaC) arrangements. All these p-heptaB and p-heptaC have  $6\pi$  electrons and are aromatic according to the nucleus independent chemical shift (NICS). This novel bonding pattern is analyzed in terms of natural bond orbital (NBO) analysis. For virtually all possible  $B_7C_1^{1-}$ ,  $B_6C_2$ , and  $B_5C_3^{1-}$  combinations, the p-heptaB arrangements are the more stable than other type structures.

**Key Words :** Density functional theory, Planar heptacoordinate boron, Nucleus-independent chemical shift

## Introduction

Borocarbon clusters are binary compounds of boron and carbon, which are the adjacent elements in the periodic table. Boron carbide, well-known<sup>1-4</sup> in solid-state chemistry and physics, is an important non-metallic material with outstanding hardness, as well as excellent mechanical, thermal and electrical properties. Verhaegen and co-workers observed diatomic BC cluster in 1964 in a mass spectrometric study of the vapor in equilibrium with solid  $B_4C$ .<sup>5-f</sup> The ensuing studies of borocarbons involved either heating boron/carbon mixtures to high temperatures or laser evaporation of boron carbide layers.<sup>5</sup> In 1988, Becker and Dietze found that the intensities of positive and negative charged  $B_nC_m$  cluster ions generated by laser plasma indicated numerous magic numbers in the  $n+m = 2-17$  range.<sup>5-b</sup> While such laser plasma chemical reactions produce unexpected compositions, deducing their exact character requires investigating a wide range of alternative isomers in terms of energetic, geometric and electronic properties. Interpreting such unconventional experimental results poses a challenging problem to computational chemistry.<sup>35</sup> Experimentally, the products species are trapped in noble gas matrices, where various spectroscopic methods such as infrared (IR) spectroscopy and electron spin resonance (ESR) spectroscopy are applied. ESR spectroscopy data have been reported by Easley *et al.*<sup>6-a</sup> and by Knight *et al.*,<sup>6-b,c</sup> on trapped diatomic and triatomic borocarbon clusters in noble gas matrices. Analysis of the spectra was in good agreement with the theoretical predictions.<sup>6</sup> Infrared spectroscopy also has been applied to a number of small neutral, anionic, and cationic borocarbon clusters in the gas phase.<sup>5-g,7</sup> Regarding various species of small borocarbon clusters, a considerable number of *ab initio* studies, in conjunction with experiment as well as

independent of experiment, have been performed. Thus, units of the composition  $B_nC_m$  with  $n+m = 2-5$  have been studied in cationic, neutral, or anionic charge states<sup>6-8</sup> and found to adopt linear and monocyclic structures. Structures and relative stabilities of cyclic ring, scoop, and linear structures of  $B_4C_2$  and  $B_2C_4$  with  $n+m = 6$  have been reported.<sup>9</sup> The effect of doping boron to one end of  $C_m$  chains and the experimental abundance of  $B_nC_m$  ( $m < 6$ ,  $n=1,3$ ) species has been explained using Hückel and *ab initio* calculations.<sup>10</sup> Nevertheless, most of the borocarbon clusters have been examined neither experimentally nor theoretically.

Due to electron deficient nature of boron, a hypercoordinated arrangement can be expected to arise from the donation of lone-pair electron density from the ligand to an empty orbital on the boron.<sup>13</sup> Carbon is known to prefer tetrahedral bonding,<sup>19</sup> but unusual planar tetracoordinated,<sup>20</sup> three-dimensional hypercoordinated,<sup>21</sup> and planar hypercoordinated<sup>11-16</sup> structures have been predicted. Hoffmann first analyzed electronic structure of planar carbon in methane using the extended Hückel calculation,<sup>23</sup> and elucidated it is structural stability as well as the relationship between the planar and the tetrahedral arrangement.<sup>19-a</sup> There is continued interest in theoretical and experimental planar coordinated compounds of the first-row elements.

The planar hypercoordinated arrangements in borocarbon clusters were described by Schleyer and co-workers,<sup>12,14</sup> and independently by Minkin *et al.*<sup>15,16</sup> Planar hexacoordinate carbon arrangements have been proposed for species such as  $CB_6^{2-}$  and  $C_3B_4$ .<sup>12</sup> In ref. 14, for the first time a p-heptaC arrangement of  $B_7C_1^{1-}$  composition with  $D_{7h}$  symmetry was proposed to be a local minimum using state-of-the-art computational methods, but the isomers with planar hypercoordinated boron could be lower in energy than those with

planar hypercoordinate carbon. This research yielded unanticipated bonding capabilities of these central elements and suggested the existence of other types of structures. Such unconventional structures can be expected to have unusual properties and are worth further study. Minkin and co-workers also reported results on the stability of compositions,  $B_7C^{1-}$  and  $B_6C_2$ , which compared p-heptaC with monocyclic ring.<sup>15,16</sup> However, their work did not establish which structure is the stable structures. Various bonding types should be possible for borocarbon clusters.

We now report our theoretical study on such novel bonding and the most stable structure of  $B_7C_1^{1-}$ ,  $B_6C_2$ , and  $B_5C_3^{1-}$  clusters with B3LYP and highly correlated CCSD(T) methods. The natural bond orbital (NBO) analysis and nucleus independent chemical shift (NICS)<sup>27</sup> have also been applied to analyze the bonding nature and aromaticity of the investigated species.

### Computational Methods

The geometry optimizations and frequency calculations were performed at B3LYP/6-31G\*-density functional theory (DFT) with Gaussian98 program,<sup>24</sup> initially, and then refined at B3LYP/6-311+G\*. Zero-point energy (ZPE) corrections were applied in the energy evaluations. Single point calculations using the highly correlated coupled cluster theory [CCSD(T)/cc-pVTZ]<sup>26</sup> validated the accuracy of the DFT relative energies. Key structures are shown in Figures 1 for  $B_7C^{1-}$ , 2 for  $B_6C_2$ , 3 for  $B_5C_3^{1-}$ , 4 for  $B_6C_2^{1+}$ , and 5 for  $B_6C_2^{1-}$ . Relative energies, point groups, and number of imaginary (Nimag) vibrational frequencies are included.

Non-planar monocyclic and polycyclic rings, as well as cage structures, are given in the Supporting Information (A, B, and C). In Table 2, we considered the triplet states of all p-hepta arrangements to ascertain the spin state dependence of various parameters relevant for the borocarbon species studied in this work. Nucleus-independent chemical shifts (NICS),<sup>27</sup> were based on the magnetic shielding computed at 1.0 and 1.5 (Å) distances above the central atom of the planar arrangements, and computed with the gauge-independent atomic orbitals (GIAO) method<sup>34</sup> at B3LYP/6-311+G\* level.

### Results and Discussion

We first discuss the geometry of each cluster and consider the nature of the bonding of the isoelectronic analogues  $B_7C^{1-}$ ,  $B_6C_2$ , and  $B_5C_3^{1+}$  with twenty-six valence electrons.

$B_7C^{1-}$ . The anionic  $B_7C^{1-}$  clusters have various isomers with planar, monocyclic rings, polycyclic rings, and cage structures (see Figure 1). The p-heptaB structure **1**, with  $C_{2v}$  symmetry, is the most stable at both the B3LYP/6-311+G\* and CCSD(T)/cc-pVTZ levels, which has no imaginary frequency at B3LYP/6-311+G\*. The p-heptaC and p-heptaB arrangements differ fundamentally from the conventional trigonal  $sp^2$  hybridization. The central boron in p-heptaB structure **1** exhibits the multiple bonding, but the octet rule is not violated since the total Wiberg bond indices (WBI) for the central atom are 3.59 in Table 2. The WBI is a measure of the bond order based on natural bond orbital (NBO)<sup>28</sup> analysis. According to the result of the NBO analysis, the total number of  $\pi$  electron in p-heptaB arrangement **1** is six,

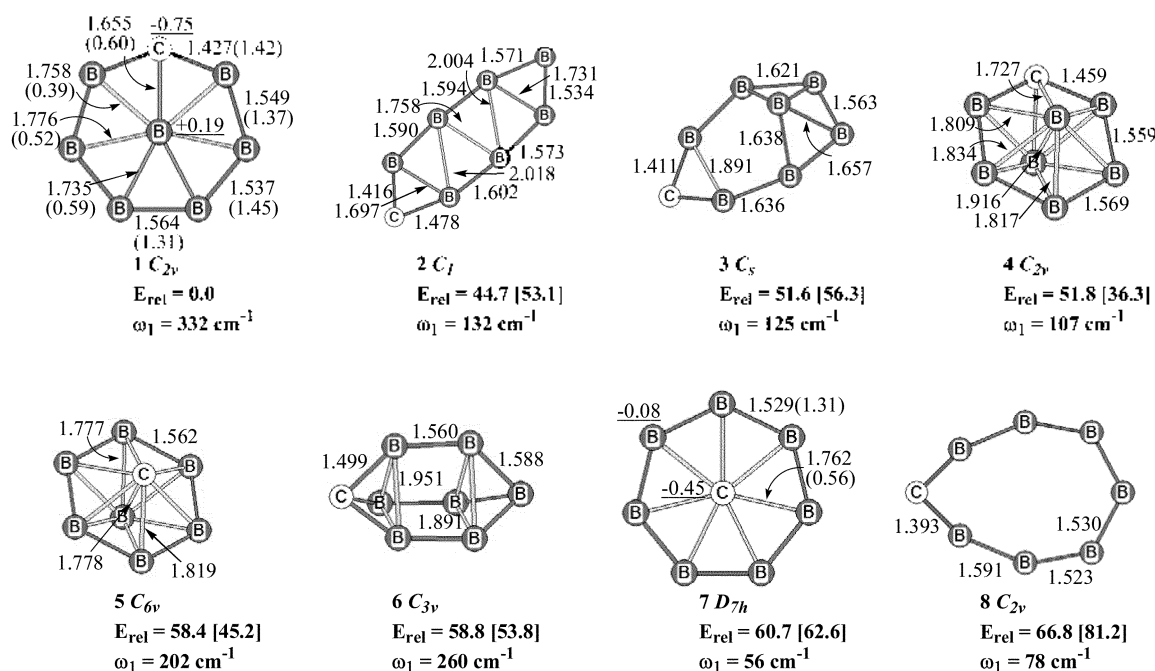


**Figure 1.** Optimized geometries, relative energies (kcal/mol), and smallest frequencies ( $\omega_1$ ) at the B3LYP/6-311+G\* on anionic  $B_7C$  potential energy surface. The WBI values are in parenthesis, the natural atomic charges are underlined, and the brackets are relative energies at the CCSD(T)/cc-pVTZ levels.

in accordance with the Hückel's  $(4n+2)\pi$  electrons rule. The natural atomic charge difference between the central and the edge atom reveals the character of the bonding. Generally, B-B, B-C, and C-C bonds are covalent, but bonds can be partially ionic in bonding character because of the difference in electronegativity between boron and carbon. Ionic contributions in covalent bonds strengthen the bonding. The central carbon in **7** ( $D_{7h}$ ) has a negative charge of  $-0.45e$  and the edge boron has a small negative charge of  $-0.08e$ . In **1** ( $C_{2v}$ ), the central boron has a positive charge of  $+0.19e$ , and the ring carbon and borons have negative charges of  $-0.75e$  and  $-0.07e$ , respectively. As a result, the B-C bond length to ring atom of p-heptaB in **1** is 1.655 Å and thus shorter than 1.762 Å in **7**. The p-heptaC structure **7** ( $D_{7h}$ ) is the local minimum reported by Schleyer *et al.*<sup>11</sup> at the B3LYP/6-311+G\* and by Minkin *et al.*<sup>15,16</sup> at the B3LYP/6-311+G(2df). Our optimized bond distances to the center and in the ring are 1.762 and 1.529 Å, respectively, compared with Minkin *et al.*'s, 1.755 and 1.523 Å, respectively. However, structure **7** is 60.7 kcal/mol higher in energy at B3LYP/6-311+G\* and 62.6 kcal/mol at CCSD(T)/cc-pVTZ

than the most stable structure **1**.

The chain-like structure **2** ( $C_1$ ), scoop structure **3** ( $C_1$ ), cage structures **4** ( $C_{2v}$ ), **5** ( $C_{6v}$ ), and **6** ( $C_{3v}$ ), and monocyclic ring structure **8** all are local minima at B3LYP/6-311+G\*. These are predicted to be 44.7, 51.6, 51.8, 58.4, 58.8, and 66.8 kcal/mol, respectively, higher in energy than structure **1** at the B3LYP/6-311+G\*. At the CCSD(T)/cc-pVTZ, these values are 53.1, 56.3, 36.3, 45.2, 53.8, and 81.2 kcal/mol, respectively. The bond distances of B-C and B-B are found to be in the range of normal bonding.<sup>29</sup>

**B<sub>6</sub>C<sub>2</sub>**. For the neutral  $B_6C_2$  clusters, twelve isomers have been characterized (Figure 2). Similar to the anionic  $B_7C^{1-}$  cluster, the most stable  $B_6C_2$  isomer is a p-heptaB structure **9** with  $C_{2v}$  symmetry. The average B-C and B-B bond distances in **9** measured from the center are 1.650 Å and 1.726 Å, respectively. Within the ring, B-C and B-B are 1.423 Å and 1.556 Å, respectively at the B3LYP/6-311+G\*. According to NBO analysis, as presented in Table 2, the total number of  $\pi$  electrons is 5.98 in **9**. The  $p(\pi)$  occupancy of the central boron is 0.62. In this case, the  $6\pi$  electrons are strongly delocalized on the plan of **9**. The WBIs for B-B and

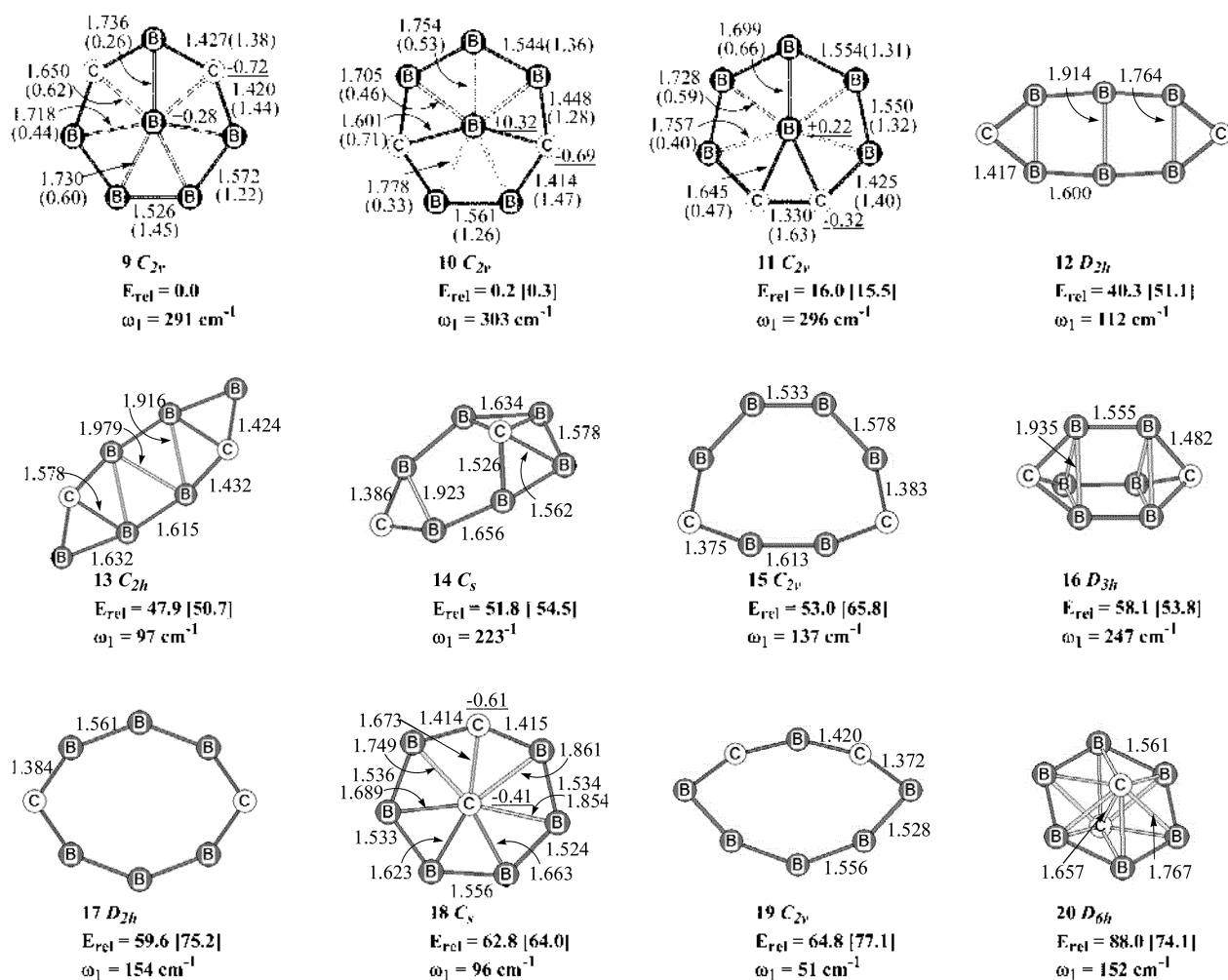


**Figure 2.** Optimized geometries, relative energies (kcal/mol), and smallest frequencies ( $\omega_1$ ) at the B3LYP/6-311+G\* on neutral  $B_6C_2$  potential energy surface. The WBI values are in parenthesis, the natural atomic charges are underlined, and the brackets are relative energies at the CCSD(T)/cc-pVTZ levels.

B-C bond in **9** have average values of 1.30 and 1.41, respectively, between a single and a double bond. The WBI of the carbon-carbon bond in benzene is 1.44 at the B3LYP/6-31G\*\*/B3LYP/6-311+G\*\*. The WBIs of the B-B and B-C bonds to the center have average values of 0.47 and 0.62, respectively. All atoms of structure **9** participate in a multicenter  $s$  bond. Both the  $6\pi$ -electron delocalization and the multicenter  $\sigma$  bonding stabilize the unusual p-heptaB structure **9**. Structure **18** ( $C_s$ ) is over 60 kcal/mol less stable than **9** both at B3LYP/6-311+G\* and at CCSD(T)/cc-pVTZ (see Figure 2).

The p-heptaB arrangements **10** ( $C_{2v}$ ) and **11** ( $C_{2v}$ ) are local minima at the B3LYP/6-311+G\*. They are predicted to be 0.2 and 16.0 kcal/mol at the B3LYP/6-311-G\*, relatively, and 0.3 and 15.5 kcal/mol at the CCSD(T)/cc-pVTZ, respectively, higher in energy than **9**. Geometrically, the structures of **10** and **11** are similar to their counterpart structure **9**.

The Other structures, chain-like structures **12** ( $D_{2h}$ ) and **13** ( $C_{2h}$ ), monocyclic ring **15** ( $C_{2v}$ ), **17** ( $C_s$ ), and **19** ( $C_{2v}$ ), scoop **14** ( $C_s$ ), and cage **16** ( $D_{3h}$ ) and **20** ( $D_{6h}$ ) are local minima.

Chain-like structures **12** ( $D_{2h}$ ) and **13** ( $C_{2h}$ ) are 40.3 and 47.9 kcal/mol, respectively, higher in energy than **9** at B3LYP/6-311+G\*. At the CCSD(T)/cc-pVTZ, the values are 51.1 and 50.7 kcal/mol. The relationships among monocyclic ring structures **15** ( $C_{2v}$ ), **17** ( $C_s$ ), and **19** ( $C_{2v}$ ) agree well with the results of Minkin *et al.*<sup>15</sup> and lie 53.0, 59.6, and 64.8 kcal/mol, respectively, in energy above the structure **9** at the B3LYP/6-311+G\*. Scoop **14** ( $C_s$ ), cage **16** ( $D_{3h}$ ) and **20** ( $D_{6h}$ ) are similar to their anionic  $B_7C^-$  counterparts. The scoop **14** ( $C_s$ ) is 51.8 kcal/mol less stable than **9** at the B3LYP/6-311-G\*, and is close in energy to the monocyclic ring **15** ( $C_{2v}$ ). The corresponding energies at the CCSD(T)/cc-pVTZ are mostly the same. The three-dimensional cage structure **16** ( $D_{3h}$ ) and **20** ( $D_{6h}$ ), composed of two pyramids and two 6-folded scoops, respectively, are 58.1 and 88.0 kcal/mol, respectively, at the B3LYP/6-311+G\* and 53.8 and 74.1 kcal/mol, respectively, at the CCSD(T)/cc-pVTZ higher in energy than the most stable structure **9**.

$B_5C_3^{1+}$ . For the cationic  $B_5C_3^{1+}$  clusters, Figure 3 describes the structures of twelve minima with different stationary states. All geometries were optimized at the B3LYP/6-

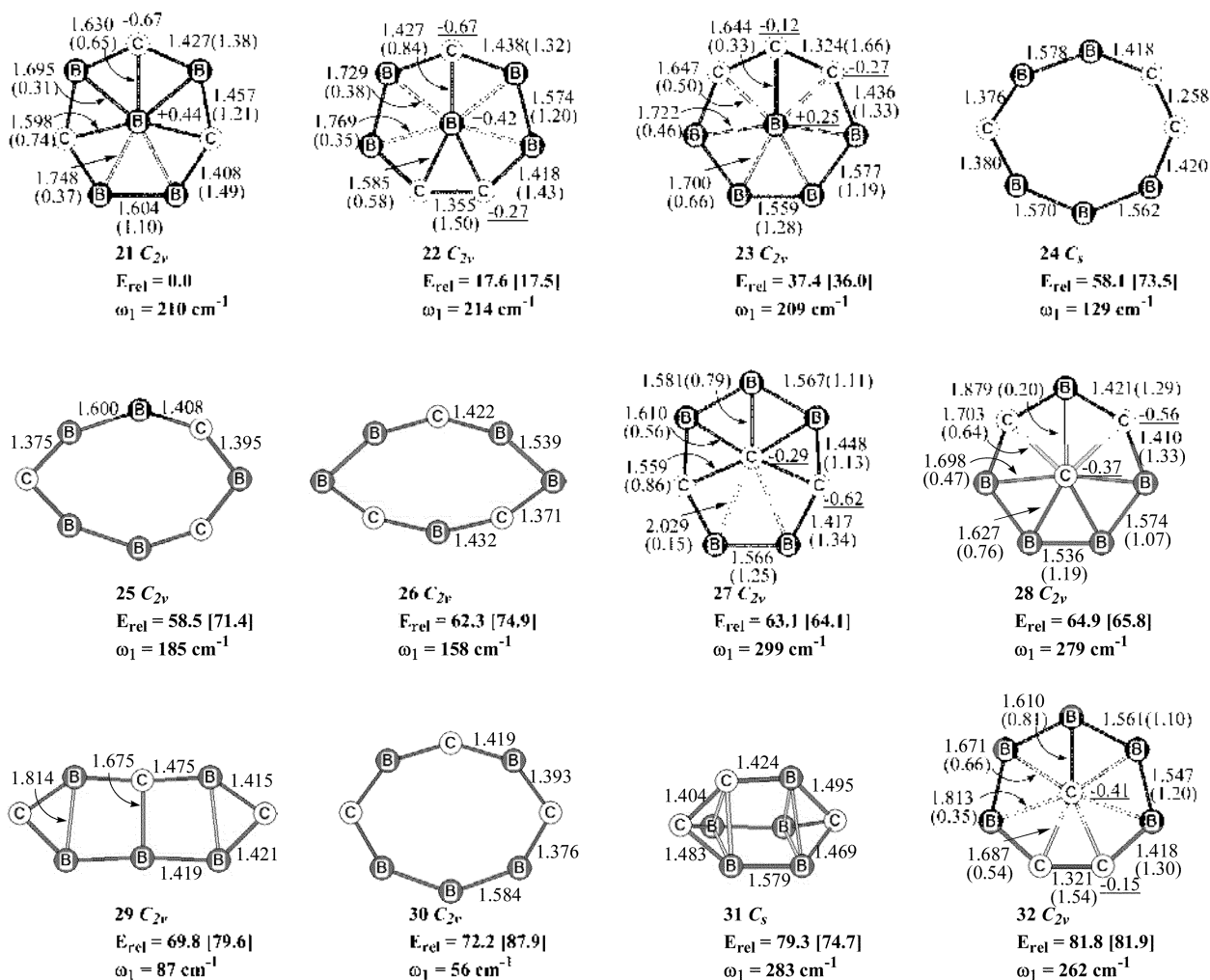


**Figure 3.** Optimized geometries, relative energies (kcal/mol), and smallest frequencies ( $\omega_1$ ) at the B3LYP/6-311+G\* on anionic  $B_5C_3^-$  potential energy surface. The WBI values are in parenthesis, the natural atomic charges are underlined, and the brackets are relative energies at the CCSD(T)/cc-pVTZ.

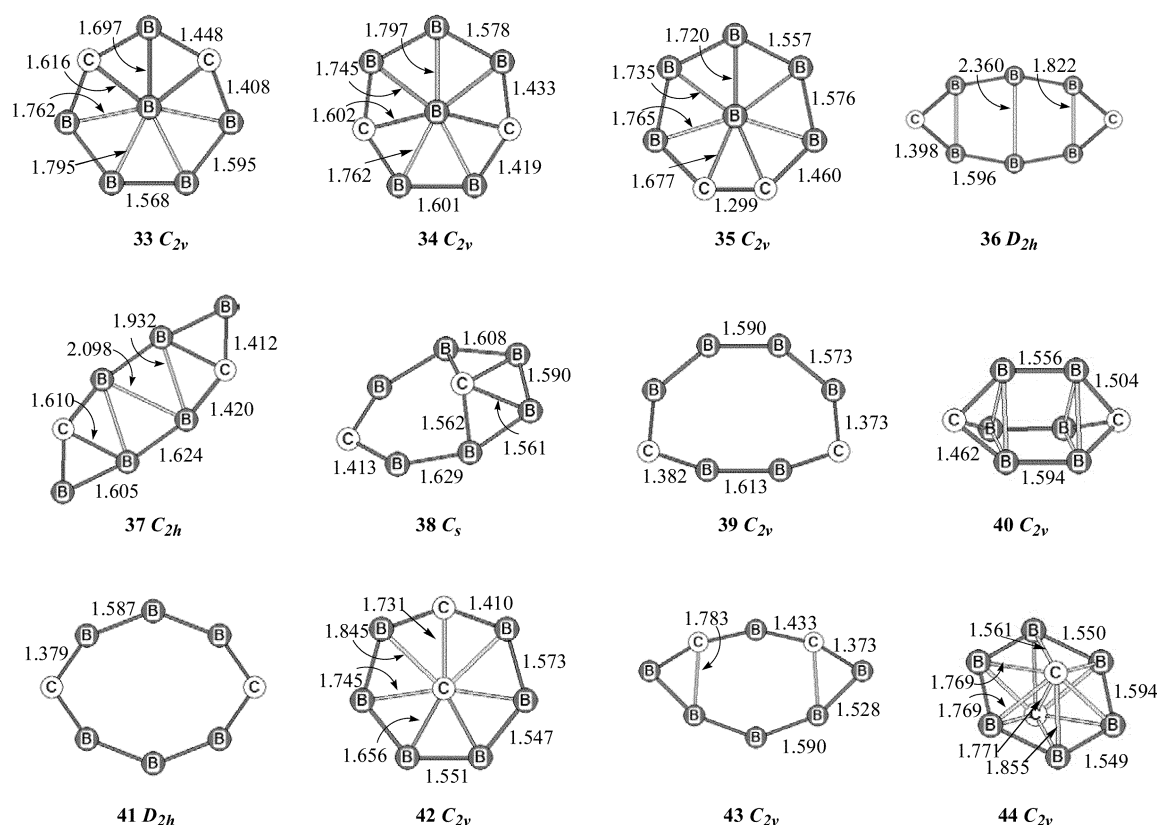
**Table 1.** Ionization Potentials and Electron Affinities of the Neutral  $B_6C_2$  Isomers at B3LYP/6-311+G\* Level

| Isomers | Ionization Potential |                  | Electron Affinity |                  | Isomers | Ionization Potential |                  | Electron Affinity |                  |
|---------|----------------------|------------------|-------------------|------------------|---------|----------------------|------------------|-------------------|------------------|
|         | AIP <sup>a</sup>     | VIP <sup>b</sup> | AEA <sup>a</sup>  | VEA <sup>b</sup> |         | AIP <sup>a</sup>     | VIP <sup>b</sup> | AEA <sup>a</sup>  | VEA <sup>b</sup> |
| 9       | 8.64                 | 8.77             | 1.38              | 0.71             | 15      | 8.09                 | 8.23             | 3.31              | 3.14             |
| 10      | 8.27                 | 8.35             | 1.08              | 0.73             | 16      | 8.24                 | 8.56             | 1.97              | 1.49             |
| 11      | 8.73                 | 8.83             | 0.96              | 0.63             | 17      | 7.78                 | 7.86             | 2.86              | 2.49             |
| 12      | 8.55                 | 8.90             | 2.46              | 2.08             | 18      | 8.08                 | 8.17             | 0.43              | 0.23             |
| 13      | 7.37                 | 7.44             | 2.44              | 2.31             | 19      | 7.52                 | 7.76             | 2.84              | 2.44             |
| 14      | 8.90                 | 9.40             | 2.51              | 2.08             | 20      | 9.64                 | 9.80             | 0.56              | -0.03            |

<sup>a</sup>Adiabatic IP and EA. <sup>b</sup>Vertical IP and EA.

311+G\* and determined to be minima by vibrational frequency computations. These geometries show an arrangement of atoms similar to those of the corresponding structures of anionic  $B_7C^{1-}$  and neutral  $B_6C_2$  clusters. Structure **21** with  $C_{2v}$  symmetry is the most stable among all of the isomers investigated. The average bond distances of the three B-C bonds and the four B-B bonds from the center are 1.609 Å and 1.722 Å, respectively. The central boron in the p-hepta structure **21** has multiple connected systems, and a total WBI for the central atom is 3.48 (Table 2). The WBIs of the B-C and B-B ring bonds in **21** have average values of 1.36 and 1.10, respectively. The WBIs of the B-C and B-B bonds to the center are 0.71 and 0.34 on average, respectively, demonstrating the multi-centered bonding principle realized in these units. The NBO  $\rho(\pi)$  occupancy of the central boron is 0.61. Like the anionic  $B_7C^{1-}$  and neutral

$B_6C_2$  p-heptaB structures, cyclic  $\pi$  electron delocalization in p-heptaB structure **21** is evident. The central boron of **21** has a positive natural charge of +0.44e, and ring carbons and borons have average negative charges of -0.67e and positive charges of +0.64e, respectively. Although the p-heptaB structure **22** ( $C_{2v}$ ) and **23** ( $C_{2v}$ ) show geometrical properties similar to those of the corresponding p-heptaB structure **21**, they are predicted to be 17.6 and 37.4 kcal/mol, respectively, higher in energy than **21** at the B3LYP/6-311+G\* level. At the CCSD(T)/cc-pVTZ level, these values are 17.5 and 36.0 kcal/mol, respectively. The monocyclic ring structures **24** ( $C_1$ ), **25** ( $C_{2v}$ ), **26** ( $C_{2v}$ ), and **30** ( $C_{2v}$ ) are similar in arrangement to their neutral  $B_6C_2$  counterparts, and the bond distances are very closed in each range between a single and a double bond.<sup>31</sup> These structures are local minima but the relative energies are higher 58.1, 58.5, 62.3, and 72.2 kcal/

**Figure 4.** Optimized geometries of cationic  $B_6C_2^+$  at the UB3LYP/6-311+G\*.

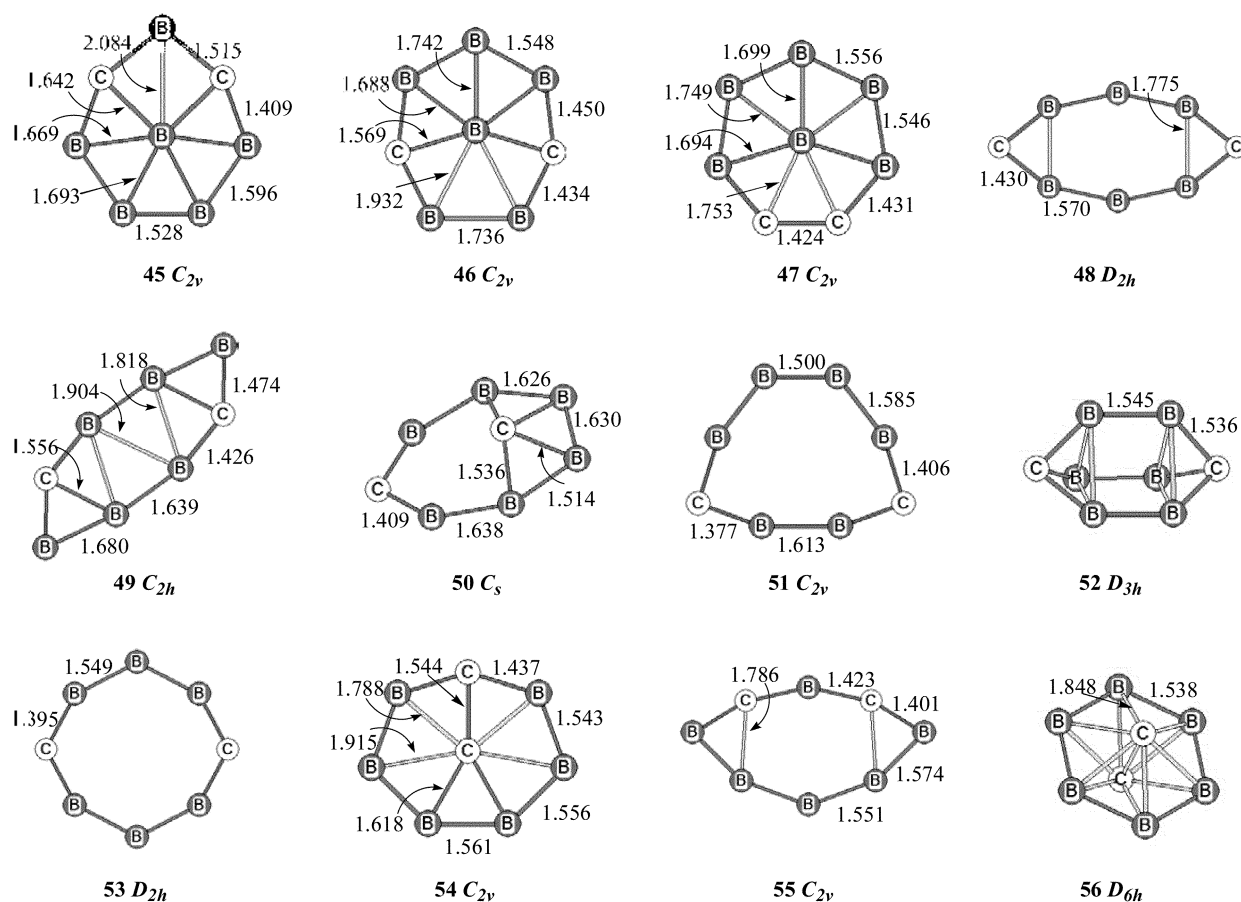


**Figure 5.** Optimized geometries of cationic  $B_6C_2^+$  at the UB3LYP/6-311+G\*.

mol, respectively, than p-heptaB structure **21** at the B3LYP/6-311+G\*. At the CCSD(T)/cc-pVTZ, the values are 73.5, 71.4, 74.9, and 87.9 kcal/mol, respectively. The p-heptaC structures **27** ( $C_{2v}$ ), **28** ( $C_{2v}$ ), and **32** ( $C_{2v}$ ) are characterized as local minima, which are predicted to be 63.1, 64.9, and 81.8 kcal/mol, respectively, at the B3LYP/6-311+G\* and 64.1, 65.8, and 81.9 kcal/mol, respectively, at the CCSD(T)/cc-pVTZ higher in energy than the p-heptaB structure **21**. The bond distances to the central atom of the planar molecules explain indirectly that the p-heptaC arrangements (**27**, **28**, **32**) exhibit to be sterically wider than p-heptaB (**21**, **22**, **23**).

The chain-like structure **29** ( $C_{2v}$ ) and cage structure **31** ( $C_s$ ) lie 69.8 and 79.3 kcal/mol higher in energy, respectively, than the most stable structure **21** at the B3LYP/6-311+G\* and the values at the CCSD(T)/cc-pVTZ are 79.6 and 74.7 kcal/mol, respectively. The structures **29** and **31** are predicted to be the local minima, by vibrational frequency computation at the B3LYP/6-311+G\*. The interatomic bond distances in **29** and **31** were obtained structures with normal bond range (single, double, and triple bonding).<sup>29</sup>

**Ionization Potential (IP) and Electron Affinity (EA).** In Table 1, we list the IPs and EAs for the various isomers of  $B_6C_2$ . Corresponding geometries and symmetries, for cationic  $B_6C_2^+$  and anionic  $B_6C_2^-$ , optimized at UB3LYP/6-311+G\* are shown Figure 4 and Figure 5. IP and EA of atoms and

molecules are fundamental properties, as they influence, for instance, the chemical bonding characteristics and hardness of species.<sup>30</sup> We computed the adiabatic ionization potential (AIP) as the difference between the total energies of the optimized cations and the optimized neutrals, and the adiabatic electron affinity (AEA) as the difference between the total energies of the optimized neutrals and the optimized anions. The AIPs and AEAs are predicted to range from 7.37 to 9.64 eV, and from 0.43 to 3.31 eV, respectively. The AIPs of the monocyclic ring structures (**15**, **17**, and **19**) are lower than other types of structures such as planar and cage and AEAs are higher than other types of structures. The AIPs of the cage structures (**16** and **20**) are higher than other types of structures. The AEAs of p-hepta structures (**9**, **10**, **11**, and **18**) are lower than other types of structures except for cage structure **20**. The computed AIPs and AEAs compare reasonably well with experimental data of borocarbon,<sup>31</sup> boron,<sup>32</sup> and carbon<sup>33</sup> clusters by the size effects (Figure 6). Comparison of the IP in Figure 6 reveals size effects. The vertical ionization potential (VIP) is the difference between the total energies of the optimized neutral and cation at the optimized neutral geometry. The vertical electron affinity (VEA) is the difference between total energies of the optimized neutral and anion at the optimized neutral geometry. Small extensions in bond lengths and angles are discernible structural rearrangements after ionization and

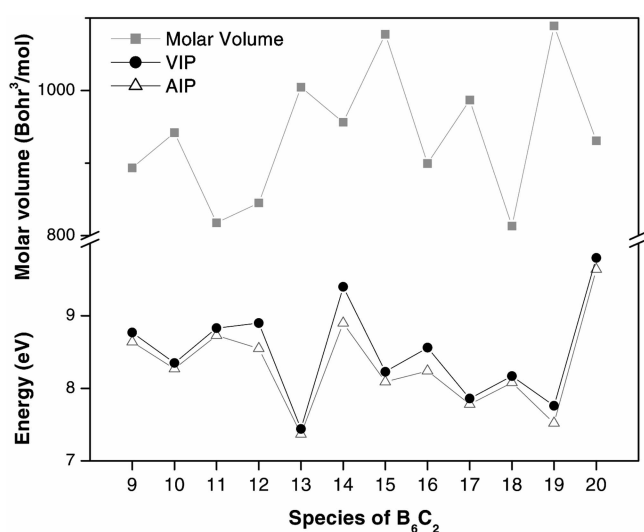


Figure 6. Molar Volume, VIP, and AIP of  $B_6C_2$  (9-20).

attaching an electron are important. However, the results of VIPs and VEAs show the same tendencies as the AIPs and AEAs (Table 1).

**HOMO-LUMO Gap.** Figure 7 displays the HOMO-LUMO gaps of all considered  $B_7C_1^-$ ,  $B_6C_2$ , and  $B_5C_3^+$  clusters at the B3LYP/6-311+G\* level, which oscillate at the

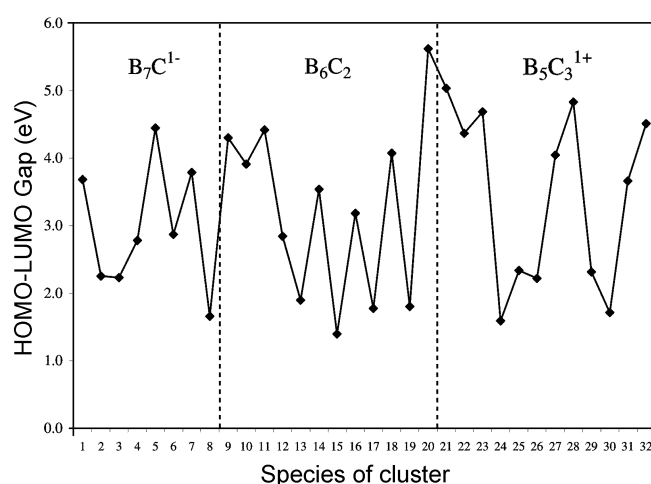


Figure 7. HOMO-LUMO Gap of  $B_7C_1^-$  (1-8),  $B_6C_2$  (9-20), and  $B_5C_3^+$  (21-32).

horizontal axis about 3.0 eV. The gaps of the p-hepta and cage structures are considerably larger than monocyclic ring and chain-like structures. These results are consistent with the ionization potentials in Table 1.

**Aromaticity of p-Hepta Structures.** Based on NICS, aromatic criteria is often definable *via* magnetic property, which has the negative NICS values (in ppm) above the

Table 2. Relative energies and Number of Imaginary (NImag) Frequencies in the Singlet and Triplet States, Total Wiberg bond Index,  $\pi$  electron occupancies, and NICS for the Compounds ( $B_7C_1^{1-}$ ,  $B_6C_2$ , and  $B_5C_3^{1+}$ )

| Species | Composition <sup>a</sup> | $\Delta E^b$ | NImag <sup>c</sup> | Tot. WBI <sup>d</sup> | Number of $\pi$ electrons <sup>e</sup> |        | NICS <sup>f</sup><br>(1.0, 1.5) Å |
|---------|--------------------------|--------------|--------------------|-----------------------|--|--------|-----------------------------------|
|         |                          |              |                    |                       | Total                                  | Center |                                   |
| 1       | $B_7C_1$ (1-,1)          | 0.0          | 0 (332)            | 3.59                  | 5.98                                   | 0.64   | (-24.2, -13.4)                    |
|         | $B_7C_1$ (1-,3)          | 64.5         | 1 (240i)           |                       |  |        |                                   |
| 7       | $B_7C_1$ (1-,1)          | 60.7         | 0 (56)             | 3.90                  | 5.97                                   | 0.93   | (-27.4, -13.5)                    |
| 9       | $B_6C_2$ (0,1)           | 0.0          | 0 (291)            | 3.56                  | 5.98                                   | 0.62   | (-23.2, -12.4)                    |
|         | $B_6C_2$ (0,3)           | 45.0         | 0 (187)            |                       |  |        |                                   |
| 10      | $B_6C_2$ (0,1)           | 0.2          | 0 (303)            | 3.52                  | 5.97                                   | 0.62   | (-23.9, -12.9)                    |
|         | $B_6C_2$ (0,3)           | 63.5         | 1 (174i)           |                       |  |        |                                   |
| 11      | $B_6C_2$ (0,1)           | 16.0         | 0 (296)            | 3.58                  | 5.98                                   | 0.68   | (-25.0, -13.4)                    |
|         | $B_6C_2$ (0,3)           | 69.4         | 1 (1112i)          |                       |  |        |                                   |
| 18      | $B_6C_2$ (0,1)           | 62.8         | 0 (96)             | 3.92                  | 5.97                                   | 1.00   | (-25.9, -12.5)                    |
|         | $B_6C_2$ (0,3)           | 112.4        | 3 (1257i)          |                       |  |        |                                   |
| 21      | $B_5C_3$ (1+,1)          | 0.0          | 0 (210)            | 3.48                  | 5.97                                   | 0.61   | (-21.3, -11.1)                    |
|         | $B_5C_3$ (1-,3)          | 67.2         | 1 (1064i)          |                       |  |        |                                   |
| 22      | $B_5C_3$ (1+,1)          | 17.6         | 0 (214)            | 3.46                  | 5.97                                   | 0.60   | (-23.7, -12.7)                    |
|         | $B_5C_3$ (1-,3)          | 70.8         | 1 (585i)           |                       |  |        |                                   |
| 23      | $B_5C_3$ (1+,1)          | 37.4         | 0 (210)            | 3.56                  | 5.97                                   | 0.71   | (-24.2, -12.6)                    |
|         | $B_5C_3$ (1-,3)          | 83.0         | 2 (279i)           |                       |  |        |                                   |
| 27      | $B_5C_3$ (1+,1)          | 63.1         | 0 (299)            | 3.94                  | 5.98                                   | 1.03   | (-23.9, -11.4)                    |
|         | $B_5C_3$ (1-,3)          | 98.1         | 1 (621i)           |                       |  |        |                                   |
| 28      | $B_5C_3$ (1+,1)          | 64.9         | 0 (279)            | 3.94                  | 5.98                                   | 1.06   | (-23.9, -11.1)                    |
|         | $B_5C_3$ (1-,3)          | 101.9        | 0 (218)            |                       |  |        |                                   |
| 32      | $B_5C_3$ (1+,1)          | 81.8         | 0 (262)            | 3.90                  | 5.98                                   | 1.07   | (-25.6, -12.2)                    |
|         | $B_5C_3$ (1-,3)          | 143.7        | 3 (676i)           |                       |  |        |                                   |

<sup>a</sup>The parentheses are charge and multiplicity. <sup>b</sup>Using the R(U)B3LYP/6-311+G\*; the energies are in kcal/mol. <sup>c</sup>Using the B3LYP/6-311+G\*; the magnitudes of smallest frequencies are in parentheses. <sup>d</sup>Total Wiberg bond indices for the central atoms and <sup>e</sup>number of  $\pi$  electron on total and central atom by NBO analysis at B3LYP/6-31G\*/B3LYP/6-31G\*. <sup>f</sup>NICS values 1.0 and 1.5 Å above the central atoms at GIAO-B3LYP/6-311+G\*.

center of clusters.<sup>27</sup> Antiaromaticity has the positive NICS values and nonaromaticity by NICS values close to zero. NICS values are calculated at 1.0 and 1.5 Å above central atoms of p-heptaB and p-heptaC structures. In Table 2, NICS values at the GIAO-B3LYP/6-311+G\* are all negative range from -21.3 to -27.4 ppm above 1.0 Å and from -11.1 to -13.5 ppm above 1.5 Å, respectively (the values above the center of benzene are -10.2 and -7.6, respectively). These results reveal the existence of delocalization and aromaticity.

**Relative Energies, Wiberg Index,  $\pi$  Electron and NICS.** As summarized in Table 2, we show the relative energies, NImag, total WBI,  $\pi$  electron occupancies, and NICS values obtained from our calculation. Although p-heptaB and p-heptaC arrangements display multiple bonding, the octet rule is not violated as documented by the total Wiberg bond indices (WBI) for the central boron and carbons which show values from 3.48 to 3.59 and from 3.90 to 3.94, respectively. The WBI is a measure of the bond order based on natural bond orbital (NBO) analysis. According to the result of NBO analysis, the total number of  $\pi$  electron in p-heptaB and p-heptaC arrangements is  $6\pi$  electrons, in keeping with Hückel's aromatic rule with  $(4n+2)\pi$  electrons. In addition, we calculated NICS values above 1.0 and 1.5 Å at central atom of p-heptaB and p-heptaC arrangements for providing a measurement of the ring current effects. Computed NICS values are all negative, suggesting the existence of delocalization and aromaticity in the twelve planar heptacoordinated species. The  $p(\pi)$  occupancy of central atom in p-heptaC, ranging from 0.93 to 1.07, is larger than that in p-heptaB, ranging from 0.60 to 0.71. In these cases, the central carbon and boron  $p(\pi)$  occupancy results from aromatic  $6\pi$  electron delocalization. The singlet states of p-hepta arrangements are confirmed to be minima, but their triplet states have one or more imaginary frequencies except for **9** and **28**. The triplet states of **9** and **28** are 45.0 and 101.9 kcal/mol, respectively, higher in energy than the corresponding singlet states at the B3LYP/6-311+G\*. We indicate the smallest frequencies for minima and the largest imaginary frequencies for non-minima.

### Conclusions

Eight  $B_7C^{1-}$ , twelve  $B_6C_2$ , and twelve  $B_5C_3^{1+}$  isomers are characterized at the B3LYP/6-311+G\* and CCSD(T)/cc-pVTZ. Besides monocyclic rings and p-heptaC isomers, unusual arrangements such as p-heptaB, scoop, and cage borocarbon clusters are considered for the first time. The most stable isomers for the anionic  $B_7C^{1-}$ , neutral  $B_6C_2$  and cationic  $B_5C_3^{1+}$  clusters have p-heptaB (**1**, **9**, and **21**, respectively) structures with  $C_{2v}$  symmetry, confirming a previous hypothesis proposed by Schleyer *et al.*<sup>14</sup> At the B3LYP/6-311+G\*, the most stable p-heptaB (**1**, **9**, and **21**) structures are in energy below the lowest isomers of the second geometric type, namely 44.7 lower than chain-like structure of  $B_7C^{1-}$  (**2**), 40.3 lower than the chain-like structure of  $B_6C_2$  (**12**), and 58.1 kcal/mol lower than monocyclic ring structure of  $B_5C_3^{1+}$  (**23**), respectively. At the CCSD(T)/

cc-pVTZ, however, the second type lowest isomers are exchanged, their relative energies with respect to the ground state energies are 36.3 for  $B_7C^{1-}$  (cage structure **4**), 50.7 for  $B_6C_2$  (chain structure **13**), and 65.8 kcal/mol in  $B_5C_3^{1+}$  (p-heptaC **27**), respectively. According to a natural atomic charge analysis of, the p-heptaB bonding is mostly polar covalent. NBO analysis suggests that strong  $\pi$  electron delocalization and multicentered  $\sigma$  bonding in p-heptaB and p-heptaC arrangements. The magnetic criterion, NICS values, has been performed for the structures, p-heptaB and p-heptaC at the GIAO-B3LYP/6-311+G\*. The resulting NICS values of twelve p-hepta structures are negative, indicating their aromaticity. Although the p-heptaB arrangement has an unusual molecular structure, it does not violate the general concepts of organic chemistry with respect to bonding properties and structural stability.  $B_7C^{1-}$ ,  $B_6C_2$ , and  $B_5C_3^{1+}$ , borocarbon clusters are predicted to adopt planar hepta-coordinated boron arrangements.

**Acknowledgement.** This work supported by Post-doctoral Fellowship Program of Korea Science & Engineering Foundation (KOSEF). I thank Professor Paul von Ragué Schleyer for helpful discussions and valuable comments about the importance of borocarbon isomers.

### References

- (a) Rao, B. K.; Jena, P. *Phys. Rev. B* **1985**, *32*, 2058. (b) Hira, S.; Ray, A. K. *Surf. Sci.* **1991**, *249*, 199.
- Aselage, T. L.; Emin, D.; McCready, S. S.; Duncan, R. V. *Phys. Rev. Lett.* **1998**, *81*, 2316.
- (a) Hall, H. T.; Compton, L. A. *Inorg. Chem.* **1965**, *4*, 1213. (b) Han, S.; Ihm, J.; Louie, S. G.; Cohen, L. *Phys. Rev. Lett.* **1999**, *80*, 995. (c) Ulrich, S.; Ehrhardt, H.; Schwan, J.; Samlenski, R.; Brenn, R. *J. Diamond Relat. Mater.* **1998**, *7*, 835. (d) McCole, I. *J. Ceramic Hardness*; Plenum: New York, 1990.
- (a) Joly, A.; Hebd, C. R. *Seances Acad. Sci.* **1883**, *97*, 456. (b) Rigdway, R. R. *Trans. Am. Electrochem. Soc.* **1934**, *66*, 117. (c) Mauri, F.; Vast, N.; Pickard, C. J. *Phys. Rev. Lett.* **2001**, *87*, 085506-1. (d) Lazzari, R.; Vast, N.; Besson, J. M.; Baroni, S.; Corso, A. D. *Phys. Rev. Lett.* **1999**, *83*, 3230. (e) Jansson, U.; Carlsson, J. *Thin Solid Films* **1985**, *124*, 101. (f) Sezer, A. O.; Brand, J. I. *Mater. Sci. Engin. B* **2001**, *79*, 191.
- (a) Becker, S.; Dietze, H.-J. *Int. J. Mass Spectrum Ion Proc.* **1986**, *73*, 157. (b) Becker, S.; Dietze, H.-J. *Int. J. Mass Spectrum Ion Proc.* **1988**, *82*, 287. (c) Wang, C.; Huang, R.; Liu, Z.; Zheng, L. *Chem. Phys. Lett.* **1995**, *242*, 355. (d) Kimura, T.; Sugai, T.; Shinohara, H. *Chem. Phys. Lett.* **1996**, *256*, 269. (e) Becker, S.; Dietze, H.-J. *J. Anal. Chem.* **1997**, *359*, 338. (f) Verhaegen, G.; Stafford, F. E.; Drowart, J. *J. Chem. Phys.* **1964**, *40*, 1622. (g) Martin, J. M. L.; Taylor, P. R.; Yustein, J. T.; Burkholder, T. R.; Andrew, L. *J. Chem. Phys.* **1993**, *99*, 12.
- (a) Easley, W. C.; Weltner, W. J. *J. Chem. Phys.* **1970**, *52*, 1489. (b) Knight, L. B.; Cobranchi, S. T.; Petty, J. T.; Earl, E.; Feller, D.; Davidson, E. R. *J. Chem. Phys.* **1989**, *90*, 690. (c) Knight, L. B.; Cabranchi, S.; Earl, E. *J. Chem. Phys.* **1996**, *104*, 4927.
- (a) Presilla-Marquez, J. D.; Larson, C. W.; Carrick, P. G.; Rittby, C. M. L. *J. Chem. Phys.* **1996**, *99*, 12. (b) Wyss, M.; Grutter, M.; Maier, J. P. *J. Phys. Chem.* **1998**, *102*, 9106. (c) Presilla-Marquez, J. D.; Carrick, P. G.; Larson, C. W. *J. Chem. Phys.* **1999**, *110*, 5702.
- (a) Kouba, J. E.; Öhrn, Y. *J. Chem. Phys.* **1970**, *53*, 3923. (b) Hirsch, G.; Buenker, R. J. *J. Chem. Phys.* **1988**, *87*, 6004. (c)



- Olipphant, N.; Adamowicz, L. *Chem. Phys. Lett.* **1990**, *168*, 126.
- (d) Fernando, W. T. M. L.; O'Brien, L. C.; Bernath, P. F. *J. Chem. Phys.* **1990**, *93*, 8482. (e) Martin, J. M. L.; Taylor, P. R. *J. Chem. Phys.* **1994**, *100*, 9002. (f) Zhan, C. G.; Iwata, S. *J. Phys. Chem.* **1997**, *101*, 591. (g) Le' onard, C.; Rosmus, P.; Wyss, M.; Maier, J. *P. Phys. Chem. Chem. Phys.* **1999**, *1*, 1827.
9. Ge, F. M.; Huang, X.; Feng, J.; Yang, C.; Sun, C. *Chem. J. Chinese Univ.* **1997**, *18*, 1838.
10. Comeau, M.; Leleyter, M.; Leclercq, J.; Pastoli, G. *Am. Inst. Phys. Conf. Proc.* **1994**, *312*, 605.
11. Havenith, R. W. A.; Fowler, P. W.; Steiner, E. *Chem. Eur. J.* **2002**, *8*, 1068.
12. Exner, K.; Schleyer, P. v. R. *Science* **2000**, *290*, 1937.
13. Griбанова, T. N.; Minyaev, R. M.; Minkin, V. I. *Mendeleev Commun.* **2001**, 169.
14. Wang, Z.-X.; Schleyer, P. v. R. *Science* **2001**, *292*, 2465.
15. Griбанова, T. N.; Minyaev, R. M.; Starikov, A. G.; Minkin, V. I. *Dokl. Akad. Nauk.* **2002**, *382*, 785.
16. Minkin, V. I.; Minyaev, R. M.; Hoffmann, R. *Russ. Chem. Rev.* **2002**, *71*, 869.
17. Pascoli, G.; Lavendy, H. *Eur. Phys. J. D* **2002**, *19*, 339.
18. (a) Kato, H.; Tanaka, E. *J. Comput. Chem.* **1991**, *12*, 1097. (b) Ray, A. K.; Howard, I. A.; Kanal, K. M. *Phys. Rev. B* **1992**, *45*, 14247. (c) Kato, H.; Yamashita, K.; Morokuma, K. *Chem. Phys. Lett.* **1992**, *190*, 361. (d) Boustani, I. *Chem. Phys. Lett.* **1995**, *240*, 135. (e) Boustani, I. *Chem. Phys. Lett.* **1995**, *233*, 273. (f) Ricca, A.; Bauschlicher, Jr., C. W. *Chem. Phys. Lett.* **1996**, *208*, 233. (g) Ricca, A.; Bauschlicher, Jr., C. W. *J. Chem. Phys.* **1997**, *106*, 2317. (h) Sowa-Resat, M. B.; Smolanoff, J.; Lapicki, A.; Anderson, S. L. *J. Chem. Phys.* **1997**, *106*, 9551. (i) Boustani, I. *Phys. Rev. B* **1997**, *55*, 16426. (j) Reis, H.; Papadopoulos, M. G.; Boustani, I. *Int. J. Quant. Chem.* **2000**, *78*, 131. (k) Aihara, J. *J. Phys. Chem. A* **2001**, *105*, 5486. (l) Li, Q. S.; Jin, H. W. *J. Phys. Chem. A* **2002**, *106*, 7042. (m) Abdurahman, A.; Shukla, A.; Seifert, G. *Phys. Rev. B* **2002**, *66*, 155423.
19. (a) van't Hoff, J. H. *Arch. Neerl. Sci. Exactes Nat.* **1874**, 445. (b) Label, J. A. *Bull. Soc. Chim. Fr.* **1874**, *22*, 337.
20. (a) Collins, J. B.; Dill, J. D.; Jemmis, E. D.; Apeloig, Y.; Schleyer, P. v. R.; Seeger, R.; Pople, J. A. *J. Am. Chem. Soc.* **1976**, *98*, 5419. (b) Luef, W.; Keese, R. *Adv. Strain Org. Chem.* **1993**, *3*, 229. (c) Sorger, K.; Schleyer, P. v. R. *J. Mol. Struct.* **1995**, *338*, 317. (d) Rottger, D.; Erker, G. *Angew. Chem., Int. Ed. Engl.* **1997**, *36*, 812. (e) Radom, L.; Rasmussen, D. R. *Pure Appl. Chem.* **1998**, *70*, 1977. (f) Boldyrev, A. I.; Simons, J. *J. Am. Chem. Soc.* **1998**, *120*, 7967. (g) Siebert, W.; Gunale, A. *Chem. Soc. Rev.* **1999**, *28*, 367. (h) Choukroun, R.; Cassoux, P. *Acc. Chem. Res.* **1999**, *32*, 494. (i) Wang, L.-S.; Boldyrev, A. I.; Li, X.; Simons, J. *J. Am. Chem. Soc.* **2000**, *122*, 7681. (j) Wang, Z.-X.; Schleyer, P. v. R. *Org. Lett.* **2001**, *3*, 1249. (k) Wang, Z.-X.; Schleyer, P. v. R. *J. Am. Chem. Soc.* **2001**, *123*, 994. (l) Wang, Z.-X.; Schleyer, P. v. R. *J. Am. Chem. Soc.* **2002**, *124*, 11979. (m) Huang, J.; Luci, J. J.; Lee, T.; Swenson, D. C.; Jensen, J. H.; Messerle, L. *J. Am. Chem. Soc.* **2003**, *125*, 1688.
21. (a) Olah, G. A.; White, A. M.; O'Brien, D. H. *Chem. Rev.* **1970**, *70*, 561. (b) Olah, G. A.; Rasul, G. *Acc. Chem. Res.* **1997**, *30*, 245.
- (c) Schleyer, P. v. R.; Würthwein, E.-U.; Kaufmann, E.; Clark, T.; Pople, J. A. *J. Am. Chem. Soc.* **1983**, *105*, 5930. (d) Kudo, H. *Nature* **1992**, *355*, 432. (e) Scherbaum, F.; Grohmann, A.; Müller, G.; Schmidbaur, H. *Angew. Chem., Int. Ed. Engl.* **1989**, *28*, 463. (f) Olah, G. A.; Rasul, G. *J. Am. Chem. Soc.* **1996**, *118*, 8503. (g) Schleyer, P. v. R.; Najafian, K. *Inorg. Chem.* **1998**, *37*, 3454. (h) Akiba, K.; Yamashita, M.; Yamamoto, Y.; Nagase, S. *J. Am. Chem. Soc.* **1999**, *121*, 10644.
22. Wang, Z.-X.; Schleyer, P. v. R. *Angew. Chem. Int. Ed.* **2002**, *41*, 4082.
23. (a) Hoffmann, R.; Alder, R. W.; Wilcox, C. F., Jr. *J. Am. Chem. Soc.* **1970**, *92*, 4992. (b) Hoffmann, R. *Pure Appl. Chem.* **1971**, *28*, 181.
24. Frisch, M. J.; Trucks, G. W.; Schlegel, H. B.; Scuseria, G. E.; Robb, M. A.; Cheeseman, J. R.; Zakrzewski, V. G.; Montgomery, J. A., Jr.; Stratmann, R. E.; Burant, J. C.; Dapprich, S.; Millam, J. M.; Daniels, A. D.; Kudin, K. N.; Strain, M. C.; Farkas, O.; Tomasi, J.; Barone, V.; Cossi, M.; Cammi, R.; Mennucci, B.; Pomelli, C.; Adamo, C.; Clifford, S.; Ochterski, J.; Petersson, G. A.; Ayala, P. Y.; Cui, Q.; Morokuma, K.; Malick, D. K.; Rabuck, A. D.; Raghavachari, K.; Foresman, J. B.; Cioslowski, J.; Ortiz, J. V.; Stefanov, B. B.; Liu, G.; Liashenko, A.; Piskorz, P.; Komaromi, I. R.; Gomperts, R.; Martin, R. L.; Fox, D. J.; Keith, T.; Al-Laham, M. A.; Peng, C. Y.; Nanayakkara, A.; Gonzalez, C.; Challacombe, M.; Gill, P. M. W.; Johnson, B.; Chen, W.; Wong, M. W.; Andres, J. L.; Gonzalez, C.; Head-Gordon, M.; Replogle, E. S.; Pople, J. A. *Gaussian 98*, revision A.5; Gaussian, Inc.: Pittsburgh, PA, 1998.
25. (a) Becke, A. D. *J. Chem. Phys.* **1993**, *98*, 5648. (b) Lee, C.; Yang, W.; Parr, R. G. *Phys. Rev. B* **1988**, *37*, 785.
26. Gauss, J. In *The Encyclopedia of Computational Chemistry*; Schleyer, P. v. R.; Allinger, N. L.; Clark, T.; Gasteiger, J.; Kollman, P. A.; Schaefer, H. F., III; Schreiner, P. R., Eds.; John Wiley & Chichester: 1998; Vol. 1, pp 615.
27. Schleyer, P. v. R.; Maerker, C.; Dransfeld, A.; Jiao, H.; Hommes, N. J. R. v. E. *J. Am. Chem. Soc.* **1996**, *118*, 6317.
28. Reed, A. E.; Curtiss, L. A.; Weinhold, F. *Chem. Rev.* **1988**, *88*, 899.
29. Typical bond length at B3LYP/6-311+G\*\* are:  $r_{CC} = 1.531$  Å in ethane, 1.396 Å in benzene, and 1.329 Å in ethene;  $r_{CB} = 1.554$  Å in  $H_3CBH_2$  and 1.376 Å in  $H_2CBH$ , and  $r_{BB} = 1.629$  Å in  $D_{2d}H_2BBH_2$  and 1.523 Å in HBBH.
30. Parr, R. G.; Yang, W. *Density-Functional Theory of Atoms and Molecules*; Oxford University Press: Oxford, 1989; pp 95-98.
31. Reid, C. J. *Int. J. Mass Spectrum Ion Proc.* **1993**, *127*, 147.
32. Hanley, L.; Whitten, J. L.; Anderson, S. L. *J. Phys. Chem.* **1988**, *92*, 5803.
33. Orden, A. V.; Saykally, R. *J. Chem. Rev.* **1998**, *98*, 2313.
34. (a) Ditchfield, R. *Mol. Phys.* **1974**, *27*, 789. (b) Wolinski, K.; Hilton, J. F.; Pulay, P. *J. Am. Chem. Soc.* **1982**, *104*, 5667. (c) Cheeseman, J. R.; Trucks, G. W.; Keith, T. A.; Frisch, M. J. *J. Chem. Phys.* **1996**, *104*, 5497.
35. (a) Park, S. S.; Lee, K. H.; Suh, Y.; Lee, C.; Luthi, H. P. *Bull. Korean Chem. Soc.* **2002**, *23*, 241.